Published in final edited form as:
Proc IEEE Inst Electr Electron Eng. 2005 April ; 93(4): 800–808. doi:10.1109/JPROC.2005.844264.

Molecular MR Imaging Probes

UMAR MAHMOOD and **LEE JOSEPHSON**
The authors are with the Center for Molecular Imaging Research, Department of Radiology, Massachusetts General Hospital, Charlestown, MA 02129 USA

Invited Paper

Magnetic resonance imaging (MRI) has been successfully applied to many of the applications of molecular imaging. This review discusses by example some of the advances in areas such as multimodality MR-optical agents, receptor imaging, apoptosis imaging, angiogenesis imaging, noninvasive cell tracking, and imaging of MR marker genes.

Keywords

Magnetic resonance imaging (MRI); *molecular imaging*; *multimodality imaging*; *optical imaging*

I. Introduction

The diverse array of rapidly growing imaging technologies detailed in this issue demonstrate the numerous approaches that are available to imaging molecular information *in vivo*. As the strengths and weaknesses of the individual methods are often complementary, no one modality will answer all biological questions. Here, magnetic resonance imaging (MRI) applications using exogenously applied imaging agents are reviewed. This review is not designed to be exhaustive but to show by example some of what is possible using MRI.

As a rule of thumb, with respect to many other whole body molecular imaging technologies, MRI has high-spatial resolution but relatively low sensitivity of detection. To improve the detectable signal changes, numerous agents including gadolinium-based small molecules [1], gadolinium-encapsulated liposomes [2], manganese-based small molecules [3], and iron oxide nanoparticles [4]-[6] have been employed. Typical detection levels of gadolinium small molecules are approximately 10^{-4} M, while the iron oxide agents have detection threshold in the 10^{-8} M range. The strength of clinical translatability for MRI-based molecular imaging approaches is seen in the fact that the imaging systems have been used hundreds of millions of times to obtain clinical images, and many of the newer molecularly selective imaging agents and techniques described here either could or have been tested in people.

II. Combination MR Optical Agents

MRI imaging agents that are observable by more than one imaging modality typically report as fluorescence with optical imaging as the second modality, while triple-labeled MR imaging agents may report with gamma rays with ^{111}In or ^{99m}Tc imaging as the third detection method. For the data acquired using each modality to be useful, the two modalities should be complementary and report either upon different molecular or physiological parameters, take advantage of different spatial resolutions, or allow feedback with different time scales while minimizing instrument complexities.

Labeling cells *ex vivo* to determine where they migrate to under normal and pathological conditions is discussed in more detail below. A number of groups have labeled cells with MRI

detectible agents, typically gadolinium-based [7]-[9] or iron oxide based [10]-[12], which are also fluorescently labeled, while others have simultaneously labeled cells with MR detectible and fluorescent agents to track their location [13]. The major advantage of dual labeling in these cases is that cellular migration may be visualized noninvasively over time by MRI, followed by histological confirmation of location at very high spatial resolution. The ability to stain these same cells for other markers including cellular differentiation markers and coregister this information with fluorescence reporting on labeled cell presence is another advantage.

Several investigators have used the fluorescence component of agents to understand at a microscopic scale the pharmacokinetics of contrast leak from the microvasculature in normal and tumoral tissues [14], [15]. In these cases, the fluorescence location and signal intensity correlate with agent delivery. An alternate paradigm has been to use the fluorescence component to report upon molecular activity and the MR component to report upon the location and concentration of probe in tissues. In particular, proteases, which are overexpressed in a variety of pathological states, can markedly increase the fluorescence of a class of “smart” optical agents [16] after cleavage of the imaging probes. This paradigm of multifold increase in fluorescence intensity after target interaction works as well with iron oxide nanoparticles as the carriers and quenchers of fluorescence [17], [18]. For example, Fig. 1 shows the draining axillary and brachial lymph nodes in a nude mouse [19]. The MRI scan shows the location of the agent in the lymph nodes as a T2 dark area, while the fluorescence intensity reflects protease activity within these nodes. Thus, the fluorescence signal in this case not only would help with intraoperative lymph node dissection after a preoperative MRI to see which nodes have normal or altered draining patterns [5], but additional *in situ* characterization based on fluorescence intensity reflecting protease activity [Fig. 1(b)] may allow increased specificity of metastatic status determination of the nodes.

An additional application of the preoperative MRI, intra-operative fluorescence imaging paradigm is in evaluating brain tumor margins [20]. Previously, it has been demonstrated that brain tumor delineation is enhanced with the use of long circulating iron oxide nanoparticles in both experimental systems [21] and in humans [22]. The multimodal nanoparticles report on the same preoperative information regarding brain tumor margins as the single modality particles [20]. However, as shown in Fig. 2, the sequestration of the particles allows relatively unencumbered near-infrared fluorescence detection instrumentation to aid the resection of tumors in the operating room, without the need for repeat intraoperative MR imaging.

III. Receptor Imaging

Imaging of receptor overexpression seen in pathology is a useful paradigm that is applicable to most imaging technologies and has been used extensively clinically with SPECT agents. The disadvantage of MRI for receptor imaging is the lower sensitivity compared to the nuclear techniques and additional barriers to quantitation of receptor density; the advantage is the markedly higher spatial resolution and associated anatomic correlation that is automatically achieved. Initial studies, more than a decade ago, using surface-modified iron oxide nanoparticles and MR to detect receptor expression, focused on highly expressed asialoglycoprotein receptors present on normal hepatocytes but not expressed on malignant hepatocellular carcinomas [23]-[25], as a differential source of contrast.

More recently, imaging of HER-2/neu receptor expression in breast cancer lines in animal models was performed using a two component gadolinium-based system [26]. The authors of the study suggest that imaging HER-2/neu receptor expression would allow status determination noninvasively and could be used to select patients who would more likely benefit from antibody therapy. Another receptor target overexpressed in a number of cancers is the folate receptor. In ovarian cancer, the folate receptor is overexpressed in the majority of cases,

and in contradistinction to HER-2/neu imaging where tumor characterization is the major goal, the goal of folate receptor imaging in ovarian cancer would be to improve detection of smaller metastatic foci and recurrence. As an example of this approach, tumor xenografts demonstrated MR contrast enhancement with gadolinium folate dendrimer administration, which was inhibited by the administration of free folic acid [27], [28].

Vascular surface targets have the advantage of fewer kinetic compartments that must be crossed for an intravenously administered contrast agent to reach its target. At sites of inflammation, endothelial adhesion molecules, such as intercellular adhesion molecule-1 and E-selectin, are upregulated. Diverse reporting moieties, including liposomes and iron oxide nanoparticles, have been used to report upon binding at sites of overexpression [29]-[32]. E-selectin overexpression has also been reported in prostate cancer epithelium itself and so may represent a more diverse target with imaging reflecting events beyond the endothelial surface [33]. Another vascular imaging target, alphaVbeta3-integrin, is upregulated in activated neovascular endothelium. Unlike the measures of angiogenesis below which reflect the vascular volume fraction and vascular leak, targets expressed in neovasculature reflect the differential rate of new vessel formation. Several groups have used gadolinium-based agents with moieties targeting alphaVbeta3 to image areas of neovasculature in tumors and atherosclerosis [34]-[36].

IV. Apoptosis

Apoptosis, programmed cell death, is a fundamental mechanism of tumor response to many types of chemotherapy. During this process, phosphatidylserine, typically present only on the inner surface of cell membranes, is exposed to the extracellular environment. The MR approaches to imaging this exposure are similar to the receptor targeting above, with phosphatidylserine as the imaging target, as schematized in Fig. 3. A major approach is to label annexin V, an endogenous human protein which recognizes this exposure. Originally, radiolabeled versions of the molecule were described [37], with subsequent testing in humans for evaluation of conditions as diverse as heart transplant rejection [38] and tumor chemotherapeutic response [39]. More recently, fluorescent versions [40], [41] have been used to evaluate apoptosis in tumors implanted in mice. Iron oxide nanoparticles coated with annexin V have been used in cell culture to image apoptosis, with increasing reduction of T2 MR signal changes correlating with increasing apoptotic fraction in cells [42]. Unlike the radio- and fluorescent-labeled annexin V, the iron oxide-based version is dominated in size by the nanoparticle; the altered blood half life and the ability to detect the particle by MRI after the local phagocytosis by host macrophages may provide a method for determining the apoptosis over a longer integral of time compared to shorter circulating detection molecules. Another approach has been to coat iron oxide nanoparticles with the C_2 domain of synaptotagmin I, which binds the membrane of apoptotic cells. Using this approach, the authors were successful in demonstrating increased binding of the conjugate, as measured by changes in MR T2 signal intensity, in tumor-bearing mice treated with chemotherapy [43]. Because of the importance of determining response to antineoplastic therapy, the approaches using MRI and other modalities will likely continue to increase.

V. Angiogenesis

Imaging of vascularity and neovascularity covers an enormous range of methods and applications in MR imaging. Numerous excellent reviews exist [44]-[47]; here, some broad themes are evaluated. A molecular-based approach to angiogenesis is to image endothelial markers overexpressed on new blood vessels using antibodies attached to MR detectable liposomes, as detailed above [34]-[36]. Characterization of lesions with respect to the vascular volume fraction or permeability of vessels provides alternate diagnostic information, and the

change in these parameters is of marked importance in the early assessment of antiangiogenic therapy. The general approaches to these characterizations include the use of small molecular gadolinium chelates, larger long circulating gadolinium-based macromolecular agents, or the use of iron oxide nanoparticles.

Dynamic imaging of small molecular gadolinium chelates allows the calculation of several kinetic and related parameters including volume transfer constant and the fractional volume of extravascular extracellular space [48], [49]. Such imaging has been used extensively to evaluate the efficacy of anti-angiogenic therapy in murine models [50]-[52]. Moreover, given the millions of doses of low molecular weight gadolinium chelates that have been routinely administered to patients, the use of such agents for calculating in humans angiogenic status of tumors before and after therapy is an attractive approach [53]-[55].

The different kinetics of gadolinium macromolecular agents allow a differing broad range of imaging sequences to be employed compared with the smaller gadolinium chelates. This may allow multiple metastatic sites to be evaluated because rapid repeat imaging is usually not required. Using such an approach, imaging signal changes correlating with vascular endothelial growth factor (VEGF) expression were seen using a macromolecular gadolinium agent; these were not apparent on nondynamic Gd-diethylene triamine pentaacetate (DTPA) imaging [56]. Changes after administration of inhibitors of VEGF were also seen as early as one day after imaging, with the use of other macromolecular gadolinium agents [57], [58]. Macromolecular gadolinium agents which at early times after administration remain in the vasculature may be combined with the subsequent administration of smaller gadolinium chelates to separate the contributions from tumoral vascular volume fraction and interstitial volume fraction [59]. Iron oxide nanoparticles have also been used in both steady state [60] and dynamically [61] to assess vascular volume fraction and endothelial transfer coefficient, respectively.

VI. Cell Tracking

The ability to track cells over time is a major strength of noninvasive molecular imaging compared to histological methods which provide higher spatial resolution but allow analysis at only one time point. Numerous fundamental biological and therapeutic questions hinge on which cells migrate to various tissues in different pathological states and how this migration may be modulated. Most of the molecular imaging modalities have techniques to track cells, either through direct labeling of cells (for example, in the case of single photon nuclear imaging techniques) or the use of stable transfection of cells with maker genes which can then report on the location of cells with the administration of an imaging agent (for example using a PET reporter or a bioluminescence reporter). Cell tracking with MRI has many advantages compared to some of the other techniques. The methods, in general, do not change viability, function, or differentiation of cells at the labeling levels typically reported [62]. The extremely high spatial resolution that can be achieved deep inside tissue compared to other modalities and the associated anatomic information regarding adjacent structures is another benefit.

Most of the MR cell tracking methods have relied on cell labeling with iron oxide nanoparticles. A major reason for this, as stated in Section I, is the lower concentration compared to small molecular paramagnetic agents needed for detection. The majority of cell labeling is performed *ex vivo* and the cells readministered either systemically or focally at the target tissue. Often, simple coincubation with nonspecific particles has been sufficient for detection, especially for cells such as macrophages that have increased phagocytic capability [63] and for cells expected to be in high concentration at a target site. The surface modification of the dextran coat of the iron oxide nanoparticles with the HIV tat peptide sequence markedly increases the uptake of the particles. This increase was up to 100-fold, compared with unmodified nanoparticles in

lymphocytes, even for early preparations [10], [11] which have been subsequently improved with respect to uptake [64]. Some investigators have used a variety of transfection agents to increase the uptake of unmodified dextran-coated iron oxide nanoparticles [65], [66], while others have used larger particles to achieve their detection threshold goals [67]. Detection thresholds in cell suspension have achieved the single cell level, initially at higher field strengths [68] and more recently at clinically standard field strengths [69]. An application-specific *in vivo* approach for cell labeling which utilized the relatively high uptake by macrophages was used to track macrophages at sites of inflammation in experimental autoimmune encephalomyelitis [70].

Cell tracking applications have included the temporal evaluation of neural or embryonic stem cell migration into regions of cerebral infarction [7], [71]. Other neurologically focused applications have included the tracking of oligodendrocyte progenitor cell migration in the spinal cord of rats [72]. Such methods should allow a more rapid rate of therapeutic optimization coupled to such cell-based treatments. Labeling of mesenchymal stem cells has likewise been utilized to track their delivery and migration in areas of myocardial infarction [73], [74]. A utility of high spatial resolution tracking over a time of T cells is the ability to determine where within a tumor systemically administered cells are delivered. As seen in Fig. 4, over the course of 36 h, cytotoxic T cells preferentially home to the tumor which expresses an antigen that they have been primed against (compared to the contralateral tumor which does not express the antigen) and, importantly, the distribution within the tumor is quite heterogeneous [75]. Additionally, because the cells were labeled with a known amount of probe, the changes in signal intensity could be correlated with cell number per voxel within the tumor.

VII. MR Marker Genes

Each of the major molecular imaging modalities has one or more marker gene strategies available which have been tested *in vivo*. The goal of marker genes is to create a method of determining when and where a gene of interest is expressed, without having a significant therapeutic effect. By coupling such a marker gene with a second gene expression that has a desired therapeutic effect, a generalizable scheme is created. A major application for such an approach is to monitor the efficacy and spatial distribution of gene therapy agent delivery. As with other applications, the spatial resolution of MRI is advantageous for observing heterogeneity of vector delivery and gene expression. To overcome the decreased sensitivity compared to isotopic approaches, a two-step procedure was developed to allow improved detection.

The transferrin receptor is a cycling receptor that is expressed by cells in conditions of low cellular iron. The transferrin receptor gene was engineered to remove the iron-regulatory region and mRNA destabilizing motifs. Thus, constitutive expression of the cell surface receptor occurs regardless of cellular iron status. However, the two atoms of serum iron attached to transferrin and which are internalized into the cell with each receptor cycle are insufficient by themselves to allow visualization of the location of engineered transferrin receptor expression noninvasively by MRI *in vivo*. A second step, coupling transferrin to iron oxide nanoparticles which have several thousand atoms of iron which are in a superparamagnetic state and which result in further changes in signal intensity when brought into proximity to one another in endosomes, allows detectability [76]. As seen in Fig. 5, two tumors, one of which was stably transfected to express the engineered transferrin receptor and the other, the identical wild type control that expressed the native transferrin receptor gene, show imagable differences in R2* relaxivity, confirmed to be secondary to differences in iron oxide nanoparticle accumulation in the stably transfected tumor. Further studies [77] have confirmed that the internalization of the nanoparticles was secondary to receptor-mediated endocytosis from the engineered

transferrin receptor. An important step for the translation of this paradigm to act as an MR marker gene was to show that the marker gene could be delivered with a viral vector delivery system and that MR marker gene expression correlated with therapeutic gene expression delivered in the same amplicon [78]. Further improvements in the transferrin-iron oxide moiety [79] have also resulted in the ability to image native levels of transferrin receptor expression in cell culture. Thus, another potential use of the imaging agent might be to provide a degree of *in situ* characterization based on transferrin receptor expression.

Another approach to MR marker gene imaging has been use of “smart agents.” This class of agents changes physically detectible properties after target interaction. Different smart probes have been developed for near-infrared optical imaging [16] and for MR imaging. One of the MR methods relies on changes in T1 relaxation as the imaging agent, EgadMe, is modified by beta-galactosidase, a common optical marker gene. In this method, the beta-galactosidase acts as an MR marker gene as well as an optical marker gene by cleaving a blocking group that shields from adjacent water the gadolinium at the center of the developed molecule [80]. This approach allowed the noninvasive observation of marker gene expression in *Xenopus* embryos. Other MR smart agents include magnetic relaxation switches [81], [82] that change their T2 relaxation properties in the presence of the target (DNA, protein, enzyme activity), by reversibly altering self-assembly of disperse magnetic particles into stable nanoassemblies. A third approach for MR smart agents takes advantage of changes in T1 relaxation times based upon changes in rotational correlation time of gadolinium as a monomer is polymerized. In this case, the MR marker is peroxidase, which results in the oligomerization [83]. Thus, a variety of marker gene and smart probes has been developed.

The noninvasive approaches that have been detailed here show some of the potential for answering biological questions *in vivo* and for determining clinical paradigms in the future. The broad diverse applications for MRI molecular imaging will continue to grow in the future as molecular biological approaches are further combined with novel imaging agents and new imaging methods.

Acknowledgements

This work was supported in part by the National Institutes of Health under Grant EB001872.

Biographies

Umar Mahmood received the B.S. degree in chemistry from Caltech and the M.D. and Ph.D. degrees from Cornell University, Ithaca, NY. His doctoral and postdoctoral work in biophysics was performed at Memorial Sloan Kettering Cancer Center and focused on tumor physiology studies using ^{31}P NMR spectroscopy. His medical residency training was in radiology at the Massachusetts General Hospital (MGH), Boston.

He is currently an Assistant Professor of Radiology, Harvard Medical School, Cambridge, MA, and Director of Small Animal Imaging at the MGH Center for Molecular Imaging Research. He enjoys using different parts of the electromagnetic spectrum, from radiowaves, to gamma rays, to image molecular events *in vivo*.

Lee Josephson received the B.S. degree in chemistry from the University of Wisconsin, Madison, and the Ph.D. degree in biochemistry from the State University of New York, Stony Brook.

During a postdoctoral fellowship in the laboratory of Dr. G. Guidotti, Harvard University, Cambridge, MA, he collaborated with Dr. L. Cantley to discover the inhibitory activity of vanadate on ATPases and phosphatases. He was a Cofounder and Chief Scientific Officer of Advanced Magnetics, Cambridge, MA, between 1982 and 1997, a company that pioneered the development of specialty magnetic materials for applications in biology and medicine. An early worker in the field of nanotechnology, he collaborated with Dr. Weissleder to demonstrate that nanoparticle-enhanced MRI could determine the metastatic status of lymph nodes in an animal model. He is currently an Associate Professor at Harvard Medical School, Cambridge. His research interests include the design and uses of magneto/optical nanoparticles, relaxation mechanisms of nanoparticle-based MR contrast agents, and imaging the effects of chemotherapy. He is a coauthor of over 60 publications and a coinventor on over 30 U.S. patents.

References

[1]. Carr DH, Brown J, Bydder GM, Steiner RE, Weinmann HJ, Speck U, Hall AS, Young IR. Gadolinium-DTPA as a contrast agent in MRI: Initial clinical experience in 20 patients. AJR Amer. J. Roentgenol 1984;143:215–224. [PubMed: 6611046]

[2]. Kabalka G, Buonocore E, Hubner K, Moss T, Norley N, Huang L. Gadolinium-labeled liposomes: Targeted MR contrast agents for the liver and spleen. Radiology 1987;163:255–258. [PubMed: 3454163]

[3]. Saeed M, Wagner S, Wendland MF, Derugin N, Finkbeiner WE, Higgins CB. Occlusive and reperfused myocardial infarcts: Differentiation with Mn-DPDP—enhanced MR imaging. Radiology 1989;172:59–64. [PubMed: 2500678]

[4]. Josephson L, Lewis J, Jacobs P, Hahn PF, Stark DD. The effects of iron oxides on proton relaxivity. Magn. Reson. Imag 1988;6:647–653.

[5]. Harisinghani MG, Barentsz J, Hahn PF, Deserno WM, Tabatabaei S, van de Kaa CH, de la Rosette J, Weissleder R. Noninvasive detection of clinically occult lymph-node metastases in prostate cancer. New England J. Med 2003;348:2491–2499. [PubMed: 12815134]

[6]. Weissleder R, Hahn PF, Stark DD, Rummeny E, Saini S, Wittenberg J, Ferrucci JT. MR imaging of splenic metastases: Ferrite-enhanced detection in rats. AJR Amer. J. Roentgenol 1987;149:723–726. [PubMed: 3498320]

[7]. Modo M, Mellodew K, Cash D, Fraser SE, Meade TJ, Price J, Williams SC. Mapping transplanted stem cell migration after a stroke: A serial, *in vivo* magnetic resonance imaging study. Neuroimage 2004;21:311–317. [PubMed: 14741669]

[8]. Modo M, Cash D, Mellodew K, Williams SC, Fraser SE, Meade TJ, Price J, Hodges H. Tracking transplanted stem cell migration using bifunctional, contrast agent-enhanced, magnetic resonance imaging. Neuroimage 2002;17:803–811. [PubMed: 12377155]

[9]. Huber MM, Staubli AB, Kustedjo K, Gray MH, Shih J, Fraser SE, Jacobs RE, Meade TJ. Fluorescently detectable magnetic resonance imaging agents. Bioconjug. Chem 1998;9:242–249. [PubMed: 9548540]

[10]. Josephson L, Tung CH, Moore A, Weissleder R. High-efficiency intracellular magnetic labeling with novel superparamagnetic-Tat peptide conjugates. Bioconjug. Chem 1999;10:186–191. [PubMed: 10077466]

[11]. Lewin M, Carlesso N, Tung CH, Tang XW, Cory D, Scadden DT, Weissleder R. Tat peptide-derivatized magnetic nanoparticles allow *in vivo* tracking and recovery of progenitor cells. Nat. Biotechnol 2000;18:410–414. [PubMed: 10748521]

[12]. Koch AM, Reynolds F, Kircher MF, Merkle HP, Weissleder R, Josephson L. Uptake and metabolism of a dual fluorochrome Tat-nanoparticle in HeLa cells. Bioconjug. Chem 2003;14:1115–1121. [PubMed: 14624624]

[13]. Crich SG, Biancone L, Cantaluppi V, Duo D, Esposito G, Russo S, Camussi G, Aime S. Improved route for the visualization of stem cells labeled with a Gd-/Eu-Chelate as dual (MRI and fluorescence) agent. Magn. Reson. Med 2004;51:938–944. [PubMed: 15122675]

[14]. Dafni H, Gilead A, Nevo N, Eilam R, Harmelin A, Neeman M. Modulation of the pharmacokinetics of macromolecular contrast material by avidin chase: MRI, optical, and inductively coupled plasma mass spectrometry tracking of triply labeled albumin. Magn. Reson. Med 2003;50:904–914. [PubMed: 14587000]

[15]. Schneider G, Seidel R, Uder M, Wagner D, Weinmann HJ, Kramann B. *In vivo* microscopic evaluation of the microvascular behavior of FITC-labeled macromolecular MR contrast agents in the hamster skinfold chamber. Invest. Radiol 2000;35:564–570. [PubMed: 10982002]

[16]. Weissleder R, Tung CH, Mahmood U, Bogdanov A Jr. *In vivo* imaging of tumors with protease-activated near-infrared fluorescent probes. Nat. Biotechnol 1999;17:375–378. [PubMed: 10207887]

[17]. Kircher MF, Weissleder R, Josephson L. A dual fluorochrome probe for imaging proteases. Bioconjug. Chem 2004;15:242–248. [PubMed: 15025519]

[18]. Kircher MF, Josephson L, Weissleder R. Ratio imaging of enzyme activity using dual wavelength optical reporters. Mol. Imag 2002;1:89–95.

[19]. Josephson L, Kircher MF, Mahmood U, Tang Y, Weissleder R. Near-infrared fluorescent nanoparticles as combined MR/optical imaging probes. Bioconjug. Chem 2002;13:554–560. [PubMed: 12009946]

[20]. Kircher MF, Mahmood U, King RS, Weissleder R, Josephson L. A multimodal nanoparticle for preoperative magnetic resonance imaging and intraoperative optical brain tumor delineation. Cancer Res 2003;63:8122–8125. [PubMed: 14678964]

[21]. Zimmer C, Weissleder R, Poss K, Bogdanova A, Wright SC Jr. Enochs WS. MR imaging of phagocytosis in experimental gliomas. Radiology 1995;197:533–538. [PubMed: 7480707]

[22]. Enochs WS, Harsh G, Hochberg F, Weissleder R. Improved delineation of human brain tumors on MR images using a long-circulating, superparamagnetic iron oxide agent. J. Magn. Reson. Imag 1999;9:228–232.

[23]. Weissleder R, Reimer P, Lee AS, Wittenberg J, Brady TJ. MR receptor imaging: Ultrasmall iron oxide particles targeted to asialoglycoprotein receptors. AJR Amer. J. Roentgenol 1990;155:1161–1167. [PubMed: 2122660]

[24]. Reimer P, Weissleder R, Brady TJ, Yeager AE, Baldwin BH, Tennant BC, Wittenberg J. Experimental hepatocellular carcinoma: MR receptor imaging. Radiology 1991;180:641–645. [PubMed: 1871273]

[25]. Josephson L, Groman EV, Menz E, Lewis JM, Bengele H. A functionalized superparamagnetic iron oxide colloid as a receptor directed MR contrast agent. Magn. Reson. Imag 1990;8:637–646.

[26]. Artemov D, Mori N, Ravi R, Bhujwalla ZM. Magnetic resonance molecular imaging of the HER-2/neu receptor. Cancer Res 2003;63:2723–2727. [PubMed: 12782573]

[27]. Konda SD, Wang S, Brechbiel M, Wiener EC. Biodistribution of a 153 Gd-folate dendrimer, generation = 4, in mice with folate-receptor positive and negative ovarian tumor xenografts. Invest. Radiol 2002;37:199–204. [PubMed: 11923642]

[28]. Konda SD, Aref M, Wang S, Brechbiel M, Wiener EC. Specific targeting of folate-dendrimer MRI contrast agents to the high affinity folate receptor expressed in ovarian tumor xenografts. Magma 2001;12:104–113. [PubMed: 11390265]

[29]. Sipkins DA, Gijbels K, Tropper FD, Bednarski M, Li KC, Steinman L. ICAM-1 expression in autoimmune encephalitis visualized using magnetic resonance imaging. J. Neuroimmunol 2000;104:1–9. [PubMed: 10683508]

[30]. Sibson NR, Blamire AM, Bernades-Silva M, Laurent S, Boutry S, Muller RN, Styles P, Anthony DC. MRI detection of early endothelial activation in brain inflammation. Magn. Reson. Med 2004;51:248–252. [PubMed: 14755648]

[31]. Kang HW, Weissleder R, Bogdanov A Jr. Targeting of MPEG-protected polyamino acid carrier to human E-selectin *in vitro*. Amino Acids 2002;23:301–308. [PubMed: 12373551]

[32]. Kang HW, Josephson L, Petrovsky A, Weissleder R, Bogdanov A Jr. Magnetic resonance imaging of inducible E-selectin expression in human endothelial cell culture. Bioconjug. Chem 2002;13:122–127. [PubMed: 11792187]

[33]. Bhaskar V, Law DA, Ibsen E, Breinberg D, Cass KM, DuBridge RB, Evangelista F, Henshall SM, Hevezi P, Miller JC, Pong M, Powers R, Senter P, Stockett D, Sutherland RL, von Freeden-Jeffry U, Willhite D, Murray R, Afar DE, Ramakrishnan V. E-selectin up-regulation allows for targeted drug delivery in prostate cancer. Cancer Res 2003;63:6387–6394. [PubMed: 14559828]

[34]. Winter PM, Morawski AM, Caruthers SD, Fuhrhop RW, Zhang H, Williams TA, Allen JS, Lacy EK, Robertson JD, Lanza GM, Wickline SA. Molecular imaging of angiogenesis in early-stage atherosclerosis with alpha(v)beta3-integrin-targeted nanoparticles. Circulation 2003;108:2270–2274. [PubMed: 14557370]

[35]. Winter PM, Caruthers SD, Kassner A, Harris TD, Chinen LK, Allen JS, Lacy EK, Zhang H, Robertson JD, Wickline SA, Lanza GM. Molecular imaging of angiogenesis in nascent Vx-2 rabbit tumors using a novel alpha(nu)beta3-targeted nanoparticle and 1.5 tesla magnetic resonance imaging. Cancer Res 2003;63:5838–5843. [PubMed: 14522907]

[36]. Sipkins DA, Cheresh DA, Kazemi MR, Nevin LM, Bednarski MD, Li KC. Detection of tumor angiogenesis *in vivo* by alphaVbeta3-targeted magnetic resonance imaging. Nat. Med 1998;4:623–626. [PubMed: 9585240]

[37]. Blankenberg FG, Katsikis PD, Tait JF, Davis RE, Naumovski L, Ohtsuki K, Kopiwoda S, Abrams MJ, Darkes M, Robbins RC, Maecker HT, Strauss HW. *In vivo* detection and imaging of phosphatidylserine expression during programmed cell death. Proc. Nat. Acad. Sci 1998;95:6349–6354. [PubMed: 9600968]

[38]. Narula J, Acio ER, Narula N, Samuels LE, Fyfe B, Wood D, Fitzpatrick JM, Raghunath PN, Tomaszewski JE, Kelly C, Steinmetz N, Green A, Tait JF, Leppo J, Blankenberg FG, Jain D, Strauss HW. Annexin-V imaging for noninvasive detection of cardiac allograft rejection. Nat. Med 2001;7:1347–1352. [PubMed: 11726976]

[39]. Belhocine T, Steinmetz N, Hustinx R, Bartsch P, Jerusalem G, Seidel L, Rigo P, Green A. Increased uptake of the apoptosis-imaging agent (99m)Tc recombinant human Annexin V in human tumors after one course of chemotherapy as a predictor of tumor response and patient prognosis. Clin. Cancer Res 2002;8:2766–2774. [PubMed: 12231515]

[40]. Petrovsky A, Schellenberger E, Josephson L, Weissleder R, Bogdanov A Jr. Near-infrared fluorescent imaging of tumor apoptosis. Cancer Res 2003;63:1936–1942. [PubMed: 12702586]

[41]. Schellenberger EA, Bogdanov A Jr. Petrovsky A, Ntziachristos V, Weissleder R, Josephson L. Optical imaging of apoptosis as a biomarker of tumor response to chemotherapy. Neoplasia 2003;5:187–192. [PubMed: 12869301]

[42]. Schellenberger EA, Bogdanov A Jr. Hogemann D, Tait J, Weissleder R, Josephson L. Annexin V-CLIO: A nanoparticle for detecting apoptosis by MRI. Mol. Imag 2002;1:102–107.

[43]. Zhao M, Beauregard DA, Loizou L, Davletov B, Brindle KM. Non-invasive detection of apoptosis using magnetic resonance imaging and a targeted contrast agent. Nat. Med 2001;7:1241–1244. [PubMed: 11689890]

[44]. Bogdanov AA, Lewin M, Weissleder R. Approaches and agents for imaging the vascular system. Adv. Drug Delivery Rev 1999;37:279–293.

[45]. McDonald DM, Choyke PL. Imaging of angiogenesis: From microscope to clinic. Nat. Med 2003;9:713–725. [PubMed: 12778170]

[46]. Daldrup-Link HE, Brasch RC. Macromolecular contrast agents for MR mammography: Current status. Eur. Radiol 2003;13:354–365. [PubMed: 12599002]

[47]. Choyke PL, Dwyer AJ, Knopp MV. Functional tumor imaging with dynamic contrast-enhanced magnetic resonance imaging. J. Magn. Reson Imag 2003;17:509–520.

[48]. Tofts PS, Brix G, Buckley DL, Evelhoch JL, Henderson E, Knopp MV, Larsson HB, Lee TY, Mayr NA, Parker GJ, Port RE, Taylor J, Weisskoff RM. Estimating kinetic parameters from dynamic contrast-enhanced T(1)-weighted MRI of a diffusable tracer: Standardized quantities and symbols. J. Magn. Reson. Imag 1999;10:223–232.

[49]. Port RE, Knopp MV, Hoffmann U, Milker-Zabel S, Brix G. Multicompartment analysis of gadolinium chelate kinetics: Blood-tissue exchange in mammary tumors as monitored by dynamic MR imaging. J. Magn. Reson. Imag 1999;10:233–241.

[50]. Robinson SP, McIntyre DJ, Checkley D, Tessier JJ, Howe FA, Griffiths JR, Ashton SE, Ryan AJ, Blakey DC, Waterton JC. Tumour dose response to the antivascular agent ZD6126 assessed by magnetic resonance imaging. Brit. J. Cancer 2003;88:1592–1597. [PubMed: 12771928]

[51]. Checkley D, Tessier JJ, Kendrew J, Waterton JC, Wedge SR. Use of dynamic contrast-enhanced MRI to evaluate acute treatment with ZD6474, a VEGF signalling inhibitor, in PC-3 prostate tumours. Brit. J. Cancer 2003;89:1889–1895. [PubMed: 14612898]

[52]. De Lussanet QG, Beets-Tan RG, Backes WH, Van Der Schaft DW, Van Engelshoven JM, Mayo KH, Griffioen AW. Dynamic contrast-enhanced magnetic resonance imaging at 1.5 Tesla with gadopentetate dimeglumine to assess the angiostatic effects of anginex in mice. Eur. J. Cancer 2004;40:1262–1268. [PubMed: 15110892]

[53]. Morgan B, Thomas AL, Drevs J, Hennig J, Buchert M, Jivan A, Horsfield MA, Mross K, Ball HA, Lee L, Mietlowski W, Fuxuis S, Unger C, O'Byrne K, Henry A, Cherryman GR, Laurent D, Dugan M, Marme D, Steward WP. Dynamic contrast-enhanced magnetic resonance imaging as a biomarker for the pharmacological response of PTK787/ZK 222584, an inhibitor of the vascular endothelial growth factor receptor tyrosine kinases, in patients with advanced colorectal cancer and liver metastases: Results from two phase I studies. J. Clin. Oncol 2003;21:3955–3964. [PubMed: 14517187]

[54]. Su MY, Cheung YC, Fruehauf JP, Yu H, Nalcioglu O, Mechetner E, Kyshtoobayeva A, Chen SC, Hsueh S, McLaren CE, Wan YL. Correlation of dynamic contrast enhancement MRI parameters with microvessel density and VEGF for assessment of angiogenesis in breast cancer. J. Magn. Reson. Imag 2003;18:467–477.

[55]. Eliat PA, Dedieu V, Bertino C, Boute VV, Lacroix J, Constans JM, De Korvin B, Vincent C, Bailly C, Joffre F, De Certaines J, Vincensini D. Magnetic resonance imaging contrast-enhanced relaxometry of breast tumors: An MRI multicenter investigation concerning 100 patients. Magn. Reson. Imag 2004;22:475–481.

[56]. Lewin M, Bredow S, Sergeyev N, Marecos E, Bogdanov A Jr. Weissleder R. *In vivo* assessment of vascular endothelial growth factor-induced angiogenesis. Int. J. Cancer 1999;83:798–802. [PubMed: 10597197]

[57]. Turetschek K, Preda A, Floyd E, Shames DM, Novikov V, Roberts TP, Wood JM, Fu Y, Carter WO, Brasch RC. MRI monitoring of tumor response following angiogenesis inhibition in an experimental human breast cancer model. Eur. J. Nucl. Med. Mol. Imag 2003;30:448–455.

[58]. Pradel C, Siauve N, Bruneteau G, Clement O, de Bazelaire C, Frouin F, Wedge SR, Tessier JL, Robert PH, Frija G, Cuenod CA. Reduced capillary perfusion and permeability in human tumour xenografts treated with the VEGF signalling inhibitor ZD4190: An *in vivo* assessment using dynamic MR imaging and macromolecular contrast media. Magn. Reson. Imag 2003;21:845–851.

[59]. Weissleder R, Cheng HC, Marecos E, Kwong K, Bogdanov A Jr. Non-invasive *in vivo* mapping of tumour vascular and interstitial volume fractions. Eur. J. Cancer 1998;34:1448–1454. [PubMed: 9849430]

[60]. Bremer C, Mustafa M, Bogdanov A Jr. Ntziachristos V, Petrovsky A, Weissleder R. Steady-state blood volume measurements in experimental tumors with different angiogenic burdens a study in mice. Radiology 2003;226:214–220. [PubMed: 12511693]

[61]. Daldrup-Link HE, Rydland J, Helbich TH, Bjornerud A, Turetschek K, Kvistad KA, Kaindl E, Link TM, Staudacher K, Shames D, Brasch RC, Haraldseth O, Rummeny EJ. Quantification of breast tumor microvascular permeability with feruglose-enhanced MR imaging: Initial phase II multicenter trial. Radiology 2003;229:885–892. [PubMed: 14576446]

[62]. Dodd CH, Hsu HC, Chu WJ, Yang P, Zhang HG, Mountz JD Jr. Zinn K, Forder J, Josephson L, Weissleder R, Mountz JM, Mountz JD. Normal T-cell response and *in vivo* magnetic resonance

imaging of T cells loaded with HIV transactivator-peptide-derived superparamagnetic nanoparticles. J. Immunol. Methods 2001;256:89–105. [PubMed: 11516758]

[63]. Weissleder R, Cheng HC, Bogdanova A, Bogdanov A Jr. Magnetically labeled cells can be detected by MR imaging. J. Magn. Reson. Imag 1997;7:258–263.

[64]. Zhao M, Kircher MF, Josephson L, Weissleder R. Differential conjugation of tat peptide to superparamagnetic nanoparticles and its effect on cellular uptake. Bioconjug. Chem 2002;13:840–844. [PubMed: 12121140]

[65]. Arbab AS, Bashaw LA, Miller BR, Jordan EK, Lewis BK, Kalish H, Frank JA. Characterization of biophysical and metabolic properties of cells labeled with superparamagnetic iron oxide nanoparticles and transfection agent for cellular MR imaging. Radiology 2003;229:838–846. [PubMed: 14657318]

[66]. Frank JA, Miller BR, Arbab AS, Zywicke HA, Jordan EK, Lewis BK, Bryant LH Jr. Bulte JW. Clinically applicable labeling of mammalian and stem cells by combining superparamagnetic iron oxides and transfection agents. Radiology 2003;228:480–487. [PubMed: 12819345]

[67]. Hinds KA, Hill JM, Shapiro EM, Laukkanen MO, Silva AC, Combs CA, Varney TR, Balaban RS, Koretsky AP, Dunbar CE. Highly efficient endosomal labeling of progenitor and stem cells with large magnetic particles allows magnetic resonance imaging of single cells. Blood 2003;102:867–872. [PubMed: 12676779]

[68]. Dodd SJ, Williams M, Suhan JP, Williams DS, Koretsky AP, Ho C. Detection of single mammalian cells by high-resolution magnetic resonance imaging. Biophys. J 1999;76:103–109. [PubMed: 9876127]

[69]. Foster-Gareau P, Heyn C, Alejski A, Rutt BK. Imaging single mammalian cells with a 1.5 T clinical MRI scanner. Magn. Reson. Med 2003;49:968–971. [PubMed: 12704781]

[70]. Rausch M, Hiestand P, Baumann D, Cannet C, Rudin M. MRI-based monitoring of inflammation and tissue damage in acute and chronic relapsing EAE. Magn. Reson. Med 2003;50:309–314. [PubMed: 12876707]

[71]. Hoehn M, Kustermann E, Blunk J, Wiedermann D, Trapp T, Wecker S, Focking M, Arnold H, Hescheler J, Fleischmann BK, Schwindt W, Buhrle C. Monitoring of implanted stem cell migration *in vivo*: A highly resolved *in vivo* magnetic resonance imaging investigation of experimental stroke in rat. Proc. Nat. Acad. Sci. USA 2002;99:16 267–16 272.

[72]. Bulte JW, Zhang S, van Gelderen P, Herynek V, Jordan EK, Duncan ID, Frank JA. Neurotransplantation of magnetically labeled oligodendrocyte progenitors: Magnetic resonance tracking of cell migration and myelination. Proc. Nat. Acad. Sci. USA 1999;96:15 256–15 261.

[73]. Hill JM, Dick AJ, Raman VK, Thompson RB, Yu ZX, Hinds KA, Pessanha BS, Guttman MA, Varney TR, Martin BJ, Dunbar CE, McVeigh ER, Lederman RJ. Serial cardiac magnetic resonance imaging of injected mesenchymal stem cells. Circulation 2003;108:1009–1014. [PubMed: 12912822]

[74]. Kraitchman DL, Heldman AW, Atalar E, Amado LC, Martin BJ, Pittenger MF, Hare JM, Bulte JW. *In vivo* magnetic resonance imaging of mesenchymal stem cells in myocardial infarction. Circulation 2003;107:2290–2293. [PubMed: 12732608]

[75]. Kircher MF, Allport JR, Graves EE, Love V, Josephson L, Lichtman AH, Weissleder R. *In vivo* high resolution three-dimensional imaging of antigen-specific cytotoxic T-lymphocyte trafficking to tumors. Cancer Res 2003;63:6838–6846. [PubMed: 14583481]

[76]. Weissleder R, Moore A, Mahmood U, Bhorade R, Benveniste H, Chiocca EA, Basilion JP. *In vivo* magnetic resonance imaging of transgene expression. Nat. Med 2000;6:351–355. [PubMed: 10700241]

[77]. Moore A, Josephson L, Bhorade RM, Basilion JP, Weissleder R. Human transferrin receptor gene as a marker gene for MR imaging. Radiology 2001;221:244–250. [PubMed: 11568347]

[78]. Ichikawa T, Hogemann D, Saeki Y, Tyminski E, Terada K, Weissleder R, Chiocca EA, Basilion JP. MRI of transgene expression: Correlation to therapeutic gene expression. Neoplasia 2002;4:523–530. [PubMed: 12407446]

[79]. Hogemann-Savellano D, Bos E, Blondet C, Sato F, Abe T, Josephson L, Weissleder R, Gaudet J, Sgroi D, Peters PJ, Basilion JP. The transferrin receptor: A potential molecular imaging marker for human cancer. Neoplasia 2003;5:495–506. [PubMed: 14965443]

[80]. Louie AY, Huber MM, Ahrens ET, Rothbacher U, Moats R, Jacobs RE, Fraser SE, Meade TJ. *In vivo* visualization of gene expression using magnetic resonance imaging. Nature Biotechnol 2000;18:321–325. [PubMed: 10700150]

[81]. Perez JM, Josephson L, O'Loughlin T, Hogemann D, Weissleder R. Magnetic relaxation switches capable of sensing molecular interactions. Nature Biotechnol 2002;20:816–820. [PubMed: 12134166]

[82]. Grimm J, Perez JM, Josephson L, Weissleder R. Novel nanosensors for rapid analysis of telomerase activity. Cancer Res 2004;64:639–643. [PubMed: 14744779]

[83]. Bogdanov A, Matuszewski L, Bremer C, Petrovsky A, Weissleder R. Oligomerization of paramagnetic substrates result in signal amplification and can be used for MR imaging of molecular targets. Mol. Imag 2001;1:16–23.

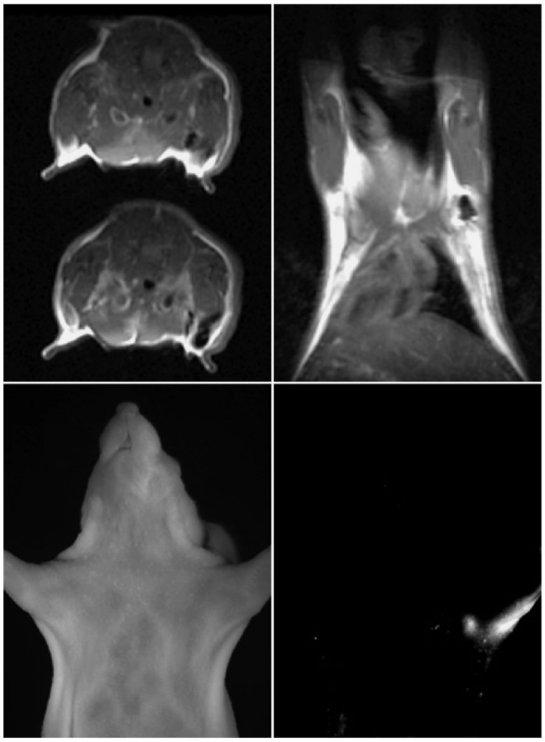

(a)

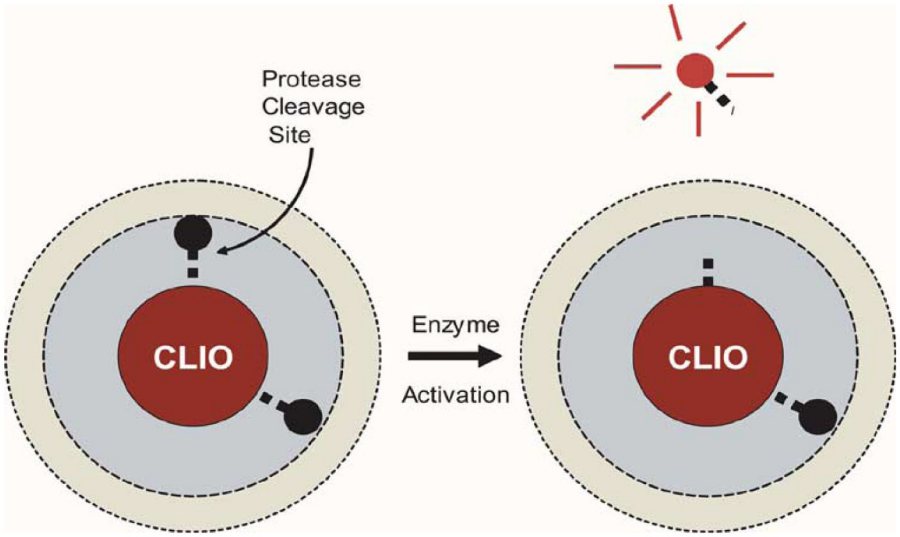

(b)

Fig. 1.

(a) Axial and coronal MRI images top and near-infrared fluorescence image bottom right. MRI-optical multimodal particle was injected into the left forepaw 24 h prior to imaging. Draining (sentinel) lymph nodes are readily seen by MRI as well as transcutaneously by fluorescence imaging (from *Bioconjug. Chem.*, vol. 13, no. 3, pp. 554-560, May-Jun. 2002, reprinted with permission). (b) Iron core partially quenches the fluorescence until the linker peptide is enzymatically cleaved by proteases and the fluorochrome is spatially separated from the core. Thus, the fluorescence signal intensity in (a) is proportional to enzyme (protease) activity within the lymph node, providing additional characterization.

Fig. 2.
MRI image (left), white light image (middle) and NIR fluorescence image (right) show a possible application of multimodal MRI-optical probes for preoperative MRI assessment and intraoperative NIR image assessment of brain tumor location and margins, allowing the radiologist and neurosurgeon to see the same lesion and same boundaries. Brain tumor is dark on T2 MRI images and is bright on NIR fluorescence images due to accumulation of probe (from *Cancer Res.*, vol. 63, no. 23, pp. 8122-8125, Dec. 2003, reprinted with permission).

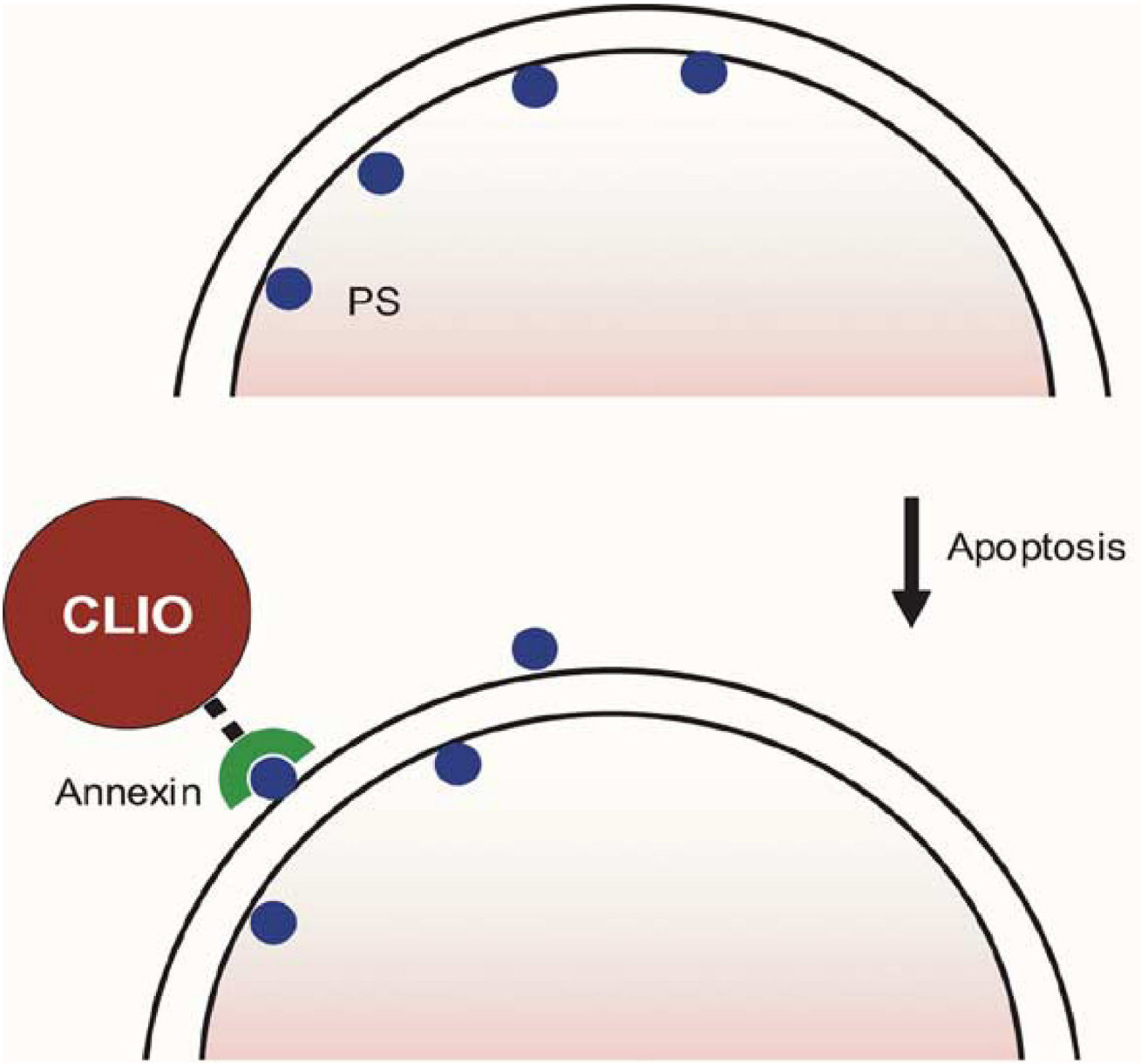

Fig. 3.
Method of MR apoptosis imaging. When cells undergo apoptosis, phosphatidylserine (PS), typically present only on the inner surface of cell membranes, is exposed to the extracellular environment. Annexin V, a human protein with a high affinity for PS, is coupled to an MRI-detectable iron oxide nanoparticle to allow visualization.

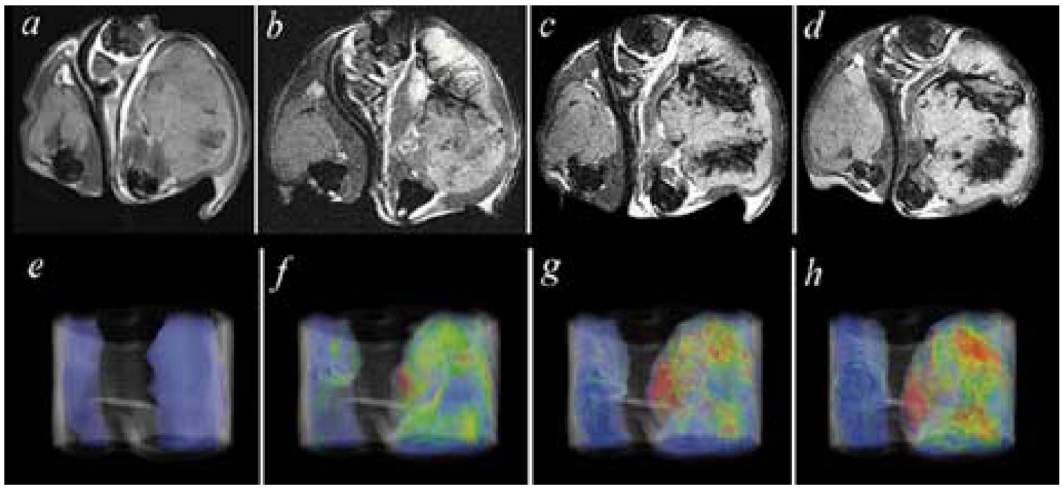

Fig. 4.

T2 weighted images (top row), and false color T2 maps (bottom row) from left to right, before, and 12, 16, and 36 h after adoptive transfer of T cells primed against an antigen expressed on the tumor in the right flank but not expressed in the tumor on the left flank of a mouse. Dark areas represent location of T cells, quantified per voxel in the bottom panel. Prior to intravenous injection, cells were labeled with an iron oxide nanoparticle, allowing their noninvasive visualization over time by MRI (from *Cancer Res.* vol. 63, no. 20, pp. 6838-6846, Oct. 2003, reprinted with permission).

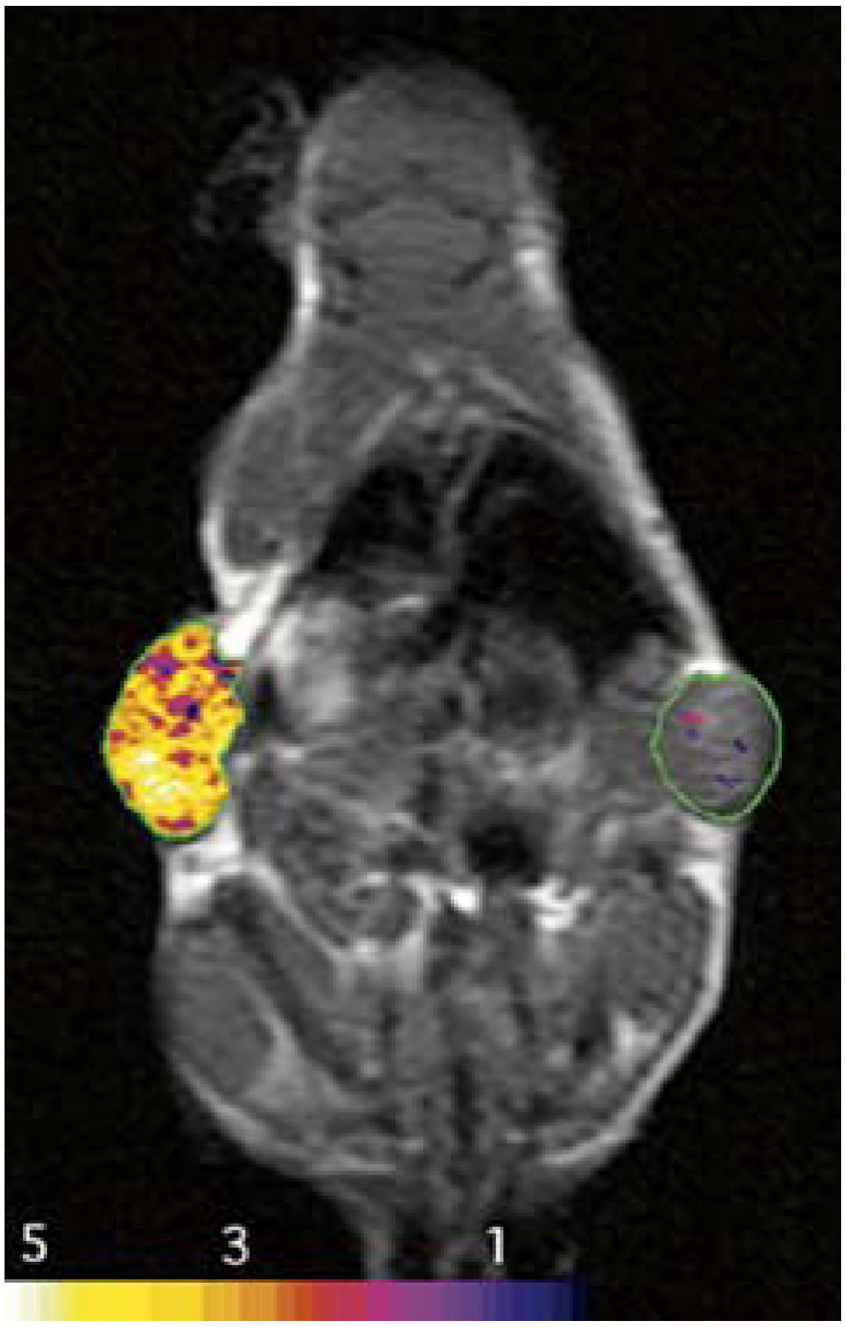

Fig. 5.

Imaging of MR marker gene expression is shown as false color R2* relaxation maps superimposed upon two tumors in this mouse. Marker gene is an engineered transferrin receptor which is constitutively expressed in the tumor on the left and not expressed in the tumor on the right. Gene expression is revealed after the administration of an iron oxide nanoparticle surface modified with transferrin. Internalization of the particle increases R2* (from *Nature Med.* vol. 6, no. 3, pp. 351-355, Mar. 2000, reprinted with permission).